

# Effect of carbon black support corrosion on the durability of Pt/C catalyst

Jiajun Wang<sup>a</sup>, Geping Yin<sup>a,\*</sup>, Yuyan Shao<sup>a,b</sup>, Sheng Zhang<sup>a</sup>, Zhenbo Wang<sup>a</sup>, Yunzhi Gao<sup>a</sup>

<sup>a</sup> *Laboratory of Electrochemistry, Department of Applied Chemistry, Harbin Institute of Technology, P.O.Box 411#, Harbin 150001, PR China*

<sup>b</sup> *Department of Macromolecular Science and Engineering, Case Western Reserve University, Cleveland, OH 44106, USA*

Received 5 May 2007; received in revised form 15 June 2007; accepted 15 June 2007

Available online 26 June 2007

## Abstract

The work intends to clarify the effect of carbon black support corrosion on the stability of Pt/C catalyst. The corrosion investigations of carbon blacks with similar structures and characteristics were analyzed by cyclic voltammograms (CV) and X-ray photoelectron spectroscopy (XPS). The results indicate that a higher oxidation degree appears on the Black Pearl 2000 (BP-2000) support, i.e. BP-2000 has a lower corrosion resistance than Vulcan XC-72 (XC-72). The durability investigation of Pt supported on the two carbon blacks was evaluated by a potential cycling test between 0.6 and 1.2 V versus reversible hydrogen electrode (RHE). A higher performance loss was observed on the Pt/BP-2000 gas diffusion electrode (GDE), compared with that of Pt/XC-72. XPS analysis suggests that higher Pt amount loss appeared in the Pt/BP-2000 GDE after durability test. X-ray diffraction (XRD) analysis also shows that Pt/BP-2000 catalyst presents a higher Pt size growth. The higher performance degradation of Pt/BP-2000 is attributed significantly to the less support corrosion resistance of BP-2000.

© 2007 Elsevier B.V. All rights reserved.

**Keywords:** PEM fuel cells; Pt/C catalyst; Carbon black; Durability; Corrosion

## 1. Introduction

Polymer electrolyte membrane fuel cell (PEMFC) is the most appropriate power source candidate for the next-generation electric vehicle and small-scale stationary power. In recent years, durability has been one of the most important issues to be solved before the commercialization of PEMFCs [1,2]. PEMFC performance loss under steady-state and cycling conditions has been attributed to the significant loss of electrochemical active surface area (EAS) of Pt catalyst [3–5], especially in the cathode where it is subjected to low pH (<1), high potential (0.6–1.2 V), high oxygen concentration, and high temperature (50–90 °C) [6]. It was found that the Pt particle agglomeration could be accelerated by both potential cycling and steady-state processes [7,8]. It has also been observed that the Pt electrode could dissolve to some extent in PEMFC operation process [9,10]. Pt dissolution–deposition and agglomeration lead to the increase of Pt particle size, which results in the decrease of the Pt EAS. Thus, the fuel cell performance is decreased.

A variety of carbon materials with high surface areas are widely used as the supports for Pt catalyst. As the catalyst support, besides the enhanced catalytic activity, the support should show good corrosion resistance because the corrosion behavior might affect the performance and stability of the Pt catalyst, especially in the cathode of PEMFC. This is because that oxygen reduction reaction occurs at potentials closer to those where oxidation of carbon can also happen. When carbon is oxidized, some Pt particles may detach from the carbon support, resulting in a decrease of catalytic activity of the catalyst. And the interaction of Pt–support may be weakened. Thus, carbon material corrosion plays a negative effect on the stability of the Pt/C catalyst. Our previous work [11,12] indicated that Pt/carbon nanotubes (CNTs) were more stable than Pt/Vulcan XC-72 (XC-72) catalyst under electrochemical operation, which can be attributed to specific interaction between Pt and the support and the higher resistance of CNTs to electrochemical oxidation. Yan and co-workers [13] also found that multi-walled carbon nanotubes (MWNTs) showed lower loss of Pt surface area and oxygen reduction reaction activity than XC-72 used as catalyst support owing to higher corrosion resistance, in agreement with our research. Despite comparative durability investigation of XC-72 and CNTs has been analyzed, this cannot provide us with the details of the effect of carbon-support corrosion on Pt catalyst

\* Corresponding author. Tel.: +86 451 86413707; fax: +86 451 86413707.

E-mail addresses: [jiajunhit@yahoo.com.cn](mailto:jiajunhit@yahoo.com.cn) (J. Wang), [yingphit@hit.edu.cn](mailto:yingphit@hit.edu.cn) (G. Yin).

stability because XC-72 and CNTs possess different structures and characteristics, which necessarily results in the difference of the two carbon materials corrosion resistance. To clarify the details of carbon support corrosion and the effect of support corrosion on the stability of Pt catalyst, it is necessary to use similar carbon materials in comparative durability study.

In this work, Black Pearls 2000 (BP-2000) and XC-72, two carbon black materials with similar structures and characteristics [14] were chosen as supports for durability study. The stabilities of the two supports and corresponding carbon supported Pt catalysts were investigated using accelerated durability test (ADT) [8,15]. The method provides a time-effective tool for evaluating the long-term performance and stability of Pt based catalyst. Furthermore, it has been developed by many researchers. Mathias et al. [16] and Makharia et al. [17] proposed the following two test methods as reliable and efficient screening tools for fuel cell catalyst development: (i) catalyst voltage cycling test; (ii) support corrosion test at 1.2 V. Since the electrochemical surface area of the fuel cell electrocatalyst decreases faster during potential cycling, which is also more closely related to drive cycle operation of PEMFC on vehicles than during constant potential or constant current testing. Borup et al. [18] also suggested potential cycling as a possible accelerated testing method for electrocatalysts. In this work, we employed the similar method to investigate the support corrosion and catalyst stability. Furthermore, the effect of carbon black support corrosion on the stability of Pt catalyst was also discussed in this paper.

## 2. Experimental

### 2.1. Preparation of Pt/C Catalyst

Pt/C catalyst was prepared by impregnation–reduction method. The detailed preparation process can be described as follows [19,20]: 30 mL water and 30 mL isopropanol were added to 50 mg carbon black, and then the suspension was ultrasonically stirred for 1 h. Thereafter, hexachloroplatinic acid ( $\text{H}_2\text{PtCl}_6$ ) was added to the suspension and ultrasonically stirred for 2 h. The pH value of the suspension was adjusted to 12 with NaOH aqueous solution, and excessive amount formaldehyde was added into the suspension. After the mixture was impregnated for 20 min, it was heated to 80 °C and then kept the agitation for 3 h at the same temperature. The resulting catalyst was washed with ultra pure water ( $\sim 18.2 \text{ M}\Omega \text{ cm}$ , Mill-Q Corp.) until  $\text{Cl}^-$  was not detected, and then dried overnight at 110 °C in vacuum.

### 2.2. Thin-film electrode preparation and durability investigation of catalyst

The catalyst electrode preparation is similar to that described by Paulus et al. [21]. An amount of the catalyst powder was dispersed in the water–methanol (1:1 volume ratio) solution to obtain a homogeneous black suspension solution. Then 5  $\mu\text{l}$  of this solution was pipetted onto the surface of a glassy carbon rotating disk electrode (0.1256  $\text{cm}^2$ , from Pine Instruments).

After the paste dried in a vacuum furnace, a drop of 5 wt% Nafion in water solution was spread on the catalyst and allowed to dry. A recast ionomer thin film covering the catalyst was thus obtained. The electrode contained about 14  $\mu\text{g cm}^{-2}$  Pt.

Electrochemical study of Pt/C catalyst was investigated on CHI 604B electrochemical working station (CH Instruments, Inc., Austin, TX). A standard three-electrode cell was employed. The glassy carbon disk covering the catalysts was used as working electrode. A piece of platinum foil of 1  $\text{cm}^2$  was served as the counter electrode and a reversible hydrogen electrode (RHE) was used as the reference electrode. Cyclic voltammogram (CV) was recorded in a 0.5  $\text{mol L}^{-1}$   $\text{H}_2\text{SO}_4$  solution. High purity argon gas was used in the experiments. Argon was passed for 30 min to eliminate oxygen. Pt catalyst corrosion test was conducted by CV between 0.60 and 1.20 V (Ar feed). Before and after the corrosion test, CV was recorded from 0.05 to 1.20 V at a scan rate of 10  $\text{mV s}^{-1}$ .

### 2.3. Corrosion investigation of carbon black support

The XC-72 and the BP-2000 carbon blacks (Cabot) were used as received. The support electrode was prepared as follows [11]: the XC-72 (or BP-2000) and PTFE emulsion (Du Pont) were suspended in isopropanol and agitated in an ultrasonic water bath, and the mixed ink was sprayed onto a PTFE hydrophobized carbon paper (Toray, containing 20 wt% PTFE), so the working electrodes were formed. The loading of spraying layer (for both XC-72 and BP-2000) was 3  $\text{mg cm}^{-2}$ , with 95 wt% carbon black and 5 wt% PTFE.

The corrosion investigation of carbon support was conducted in a three-electrode cell setup. A platinum foil and a RHE were employed as a counter and reference electrode, respectively. The above-prepared working electrode (1.0  $\times$  1.0  $\text{cm}^2$ ) was held vertically in a chamber filled with 0.5  $\text{mol L}^{-1}$   $\text{H}_2\text{SO}_4$ , with the carbon support layer exposed to the electrolyte solution. For electrochemical oxidation experiments, a constant potential of 1.2 V was applied with a HA-501 potentiostat/galvanostat (Hokuto Denko Ltd., Japan). The current density was expressed by the geometric area of the electrode. After the oxidation test, the carbon support electrode was washed with ultrapure water for several times to remove the  $\text{H}_2\text{SO}_4$  solution for further physical characterization.

### 2.4. Gas diffusion electrode (GDE) preparation and accelerated durability test (ADT)

Durability investigation of Pt/C catalyst was carried out by ADT at GDE [12], which was prepared by spraying the in-house-made Pt/XC-72 (or Pt/BP-2000, 20 wt% metal) catalysts on the poly (tetrafluoroethylene) (PTFE, DuPont) hydrophobized carbon paper (Cabot Corp.). First, the catalyst was mixed with 5 wt% Nafion ionomer solution (Electrochem. Corp.) and isopropanol in an ultrasonic bath. Then the resultant ink was sprayed onto the PTFE-hydrophobized carbon paper (20 wt% PTFE) under 40 °C. The Pt loading was 1.0  $\text{mg cm}^{-2}$ , and the content of Nafion ionomer in the catalyst layer was 10 wt% (relative to catalyst layer loading: Pt + C + Nafion ionomer).

The ADT cell consists of a three-electrode system, which included a reference electrode, a platinum mesh counter electrode and a catalyst-coated GDE as a working electrode. The above-prepared GDE ( $2.3 \times 2.3 \text{ cm}^2$ ) was held vertically in a chamber filled with  $0.5 \text{ mol L}^{-1} \text{ H}_2\text{SO}_4$ , with the catalyst layer exposed to the electrolyte solution, which mimics the environment of the electrode membrane interface in PEMFC [22]. Unlike the case of a real PEMFC, in which only the catalyst in contact with the recasted Nafion electrolyte and/or Nafion membrane is active, in the case of the ADT the entire active surface area of the electrode is exposed to the electrolyte, because the liquid electrolyte is easier access to the inside of the catalyst layer than the solid one, e.g., Nafion ionomer. Thus, the EAS is larger than that in the case of solid electrolyte and the degradation of the electrode is accelerated.

ADT was conducted by potential cycling between 0.60 and 1.20 V. CV was used to characterize the EAS, which can be determined by the charge of hydrogen adsorption/desorption region. Before ADT, the GDEs were potential-scanned between 0.05 and 1.2 V for five cycles to obtain a steady CV. After ADT, the GDEs were washed with ultra-pure water for several times to remove the  $\text{H}_2\text{SO}_4$  solution for further physical characterization.

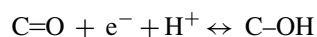
### 2.5. Physical characterization

The original sample and those scraped from post-ADT electrodes were characterized by X-ray photoelectron spectroscopy (XPS; Physical Electronics model 5700 instrument) and X-ray diffraction (XRD, Japan D/max-rB diffractometer using a  $\text{Cu K}\alpha$  X-ray source operating at 45 kV and 100 mA). The surface oxygen of the carbon support and Pt states were analyzed with XPS. The changes of Pt catalyst crystal structure and Pt mean particle size after the ADT test were determined by XRD analysis.

## 3. Results and discussion

### 3.1. Corrosion investigation of carbon black support

The electrochemical oxidation of carbon black was investigated by applying a fixed potential of 1.2 V on the both carbon electrodes, respectively. CVs for XC-72 (Fig. 1a) and BP-2000 (Fig. 1b) were recorded before and after oxidation treatment. The current density was calculated based on the electrode geometric area. It can be seen that there is an obvious current peak appears at about 0.6 V in both support electrodes, which results from the surface oxide formation due to the hydroquinone–quinone (HQ–Q) redox couple on the carbon black support surface [23–25]. The reaction corresponding to the current peaks in the HQ–Q redox region can be formulated as the following:



To demonstrate that the amount of HQ/Q redox couple increases throughout the oxidation experiment, the observed charge due to the above reaction can be calculated by subtracting the pseudo-capacitance charge from the total charge in the HQ–Q region [20]. The result is shown in Fig. 2. An obvious increase of the amount of HQ/Q redox couple can be

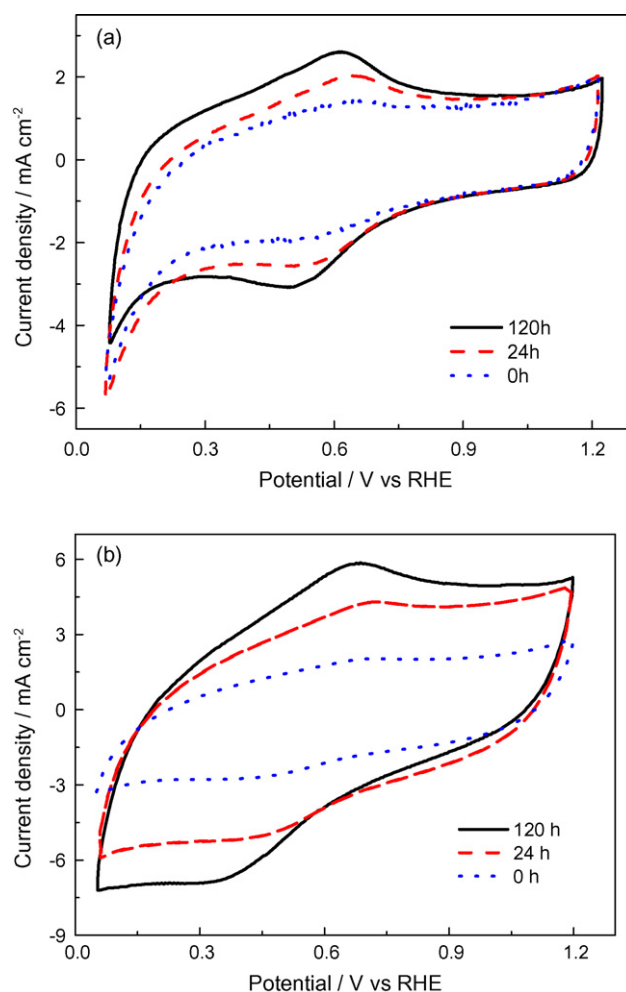


Fig. 1. Cyclic voltammograms recorded after XC-72 (a) and BP-2000 (b) electrodes hold at 1.2 V for 0, 24, and 120 h in  $0.5 \text{ mol L}^{-1} \text{ H}_2\text{SO}_4$ , scan rate:  $0.01 \text{ V s}^{-1}$ , temperature:  $20 \pm 1^\circ \text{C}$ .

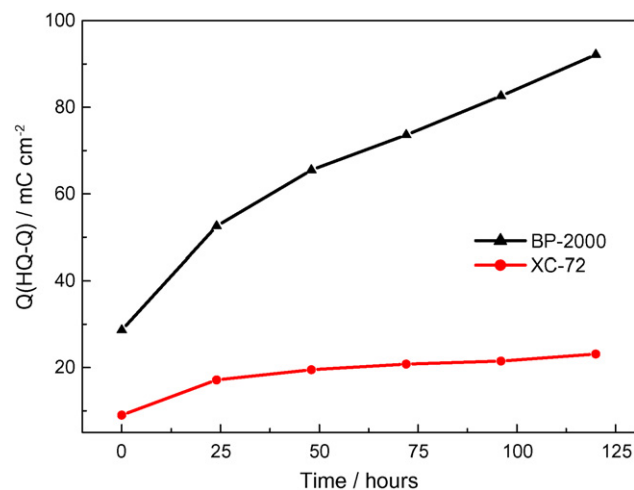


Fig. 2. The amount of the charge from HQ–Q redox as a function of hold time at 1.2 V as determined from CVs shown in Fig. 1.

observed in each sample throughout the 120 h potential hold. Furthermore, the amount of HQ/Q redox couple on the BP-2000 support electrode is enhanced by 2.2 times from 29.3 to 92.5  $\text{mC cm}^{-2}$ , while the amount on the XC-72 support electrode is enhanced only by 1.5 times from 9.3 to 23.3  $\text{mC cm}^{-2}$ . Furthermore, the amount of HQ/Q redox couple produced on the BP-2000 support ( $63.2 \text{ mC cm}^{-2}$ ) is about 4.5 times that on the XC-72 support ( $14.0 \text{ mC cm}^{-2}$ ). It is well known that the  $i_{DL}$  is proportional to the electrochemical active area of the electrode at a constant potential scan rate. From the Fig. 1, it can be seen that the double-layer current density (around 0.9 V) on BP-2000 ( $5.0 \text{ mA cm}^{-2}$ ) is about 3.1 times that on XC-72 support ( $1.6 \text{ mA cm}^{-2}$ ), which means that the electrochemical active area of BP-2000 is 3.0 times that of XC-72. Thus, it can be concluded that the increased amount of HQ/Q on BP-2000 is about 1.5 times that on XC-72 if referred to the electrochemical active area.

These results suggest that a higher oxidation degree appears on the BP 2000 support surface, i.e. XC-72 is more stable than BP-2000 under the same corrosion conditions. Also note that the above results are based on the electrochemical active area. If the amount of HQ/Q redox couple is normalized in terms of BET surface area of the carbon black support (XC-72:  $235 \text{ m}^2 \text{ g}^{-1}$  and BP-2000:  $1487 \text{ m}^2 \text{ g}^{-1}$ ) [14], the amount of HQ/Q redox couple on XC-72 electrode is higher than that of BP-2000 electrode. It seems that BP-2000 support is more stable than XC-72. It should be noted that the BET surface area is based on the power sample, not the electrode. And the measured BET surface area of BP-2000 contained significant contributions from micropores that may not be accessible to the electrolyte. Actually, the true electrochemical active surface area of BP-2000 electrode is markedly smaller than the measured BET surface area. Therefore the analysis based on BET surface area of the carbon black support is biased, and the electrochemical active area is more important to our issues, as discussed above.

XPS, which detects only the top 2–10 atom layer, has been widely used to study surface oxygen species on different carbon. In our research, the surface analysis technique was used to determine the oxygen extent on the carbon black support during corrosion test. Fig. 3 shows the survey XPS spectra XC-72 (Fig. 3a) and BP-2000 (Fig. 3b) supports before and after electrochemical oxidation at 1.2 V for 120 h in  $0.5 \text{ mol L}^{-1} \text{ H}_2\text{SO}_4$  solution. From the spectra, it can be seen that a significant increase in O 1s peak value appear in each oxidized carbon support, which is the result of higher content of surface oxides on support surface due to electrochemical oxidation. Also note that the F 1s appears on each carbon black support electrode after oxidation treatment. F 1s spectra formation comes from PTFE during the electrode preparation. Due to the existence of F 1s, it is hard to identify several oxide functional groups by deconvolution of the C 1s XPS peak. Herein what we are interested in is the total amount of the increased surface oxygen content which indicates the degree of surface oxidation. The larger the surface oxygen content, the higher oxidation degree of carbon support [26]. The surface oxygen content is determined from the O/C atomic ratio which can be obtained by integrating the area under

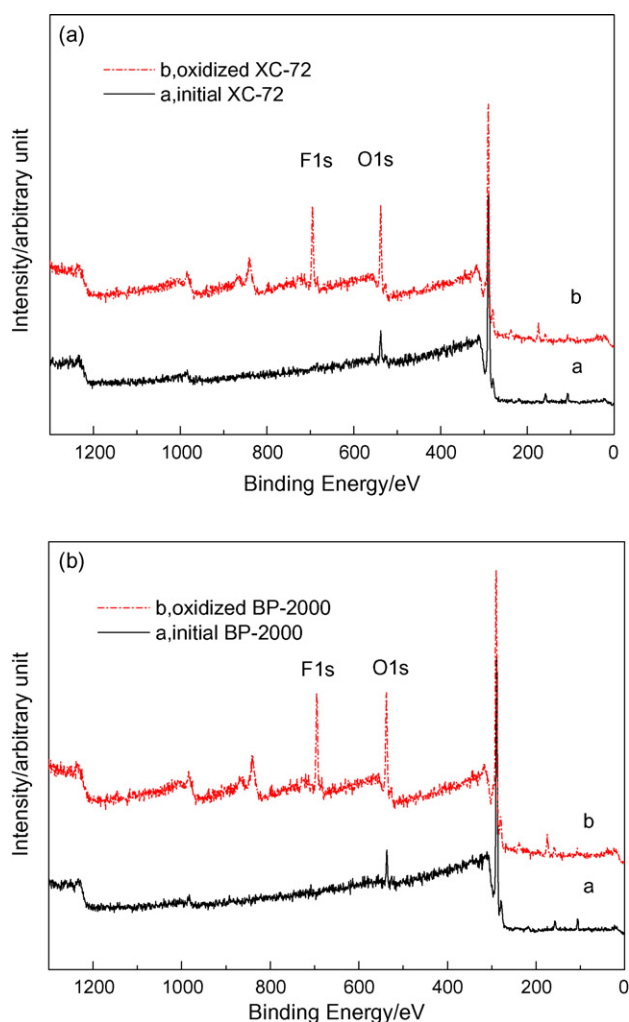


Fig. 3. Survey XPS spectra of XC-72 (a) and BP-2000 (b) supports before and after electrochemical oxidation at 1.2 V for 120 h in  $0.5 \text{ mol L}^{-1} \text{ H}_2\text{SO}_4$ .

the high-resolution XPS O 1s and C 1s spectra peaks, followed by correction with their sensitivity factors [27]. The result indicates that the O/C atomic ratio of BP-2000 support increases from 6.7% to 25.6% after oxidized treatment 120 h. By comparison, the O/C atomic ratio increases from 5.2% to 12.0% for XC-72 under the same treatment conditions, which is smaller than that of BP-2000. These results indicate that the degree of surface oxidation on BP-2000 is higher than that of XC-72.

From the CV and XPS analysis, it can be seen that BP-2000 is less resistant to electrochemical oxidation than XC-72 carbon black. Despite the two carbon black materials have similar characteristics and structures, BP-2000 possesses higher BET surface area and electrochemical active area than XC-72. Furthermore, the mesoporous area and pore volume of BP-2000 are significantly larger than those of XC-72 [14], where oxygen atom may be easy to attack. Thus, it is easy to form surface oxide species on BP-2000 carbon black. Based on the result of XPS analysis, a higher concentration of oxide species appeared on the surface of initial BP-2000 (O/C, 6.7%), compared with that of Pt/XC-72 (O/C, 5.2%). This also indicates that the BP-2000 is easier to be oxidized.

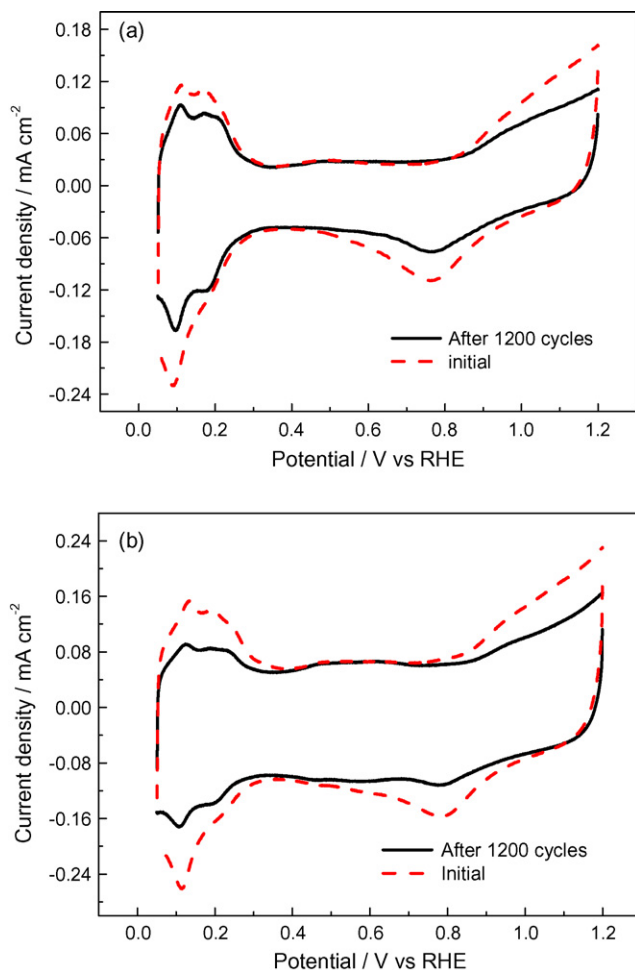


Fig. 4. Cyclic voltammograms recorded on Pt/XC-72 (a) and Pt/BP-2000 (b) thin-film electrodes before and after 1200 potential cycles, scan rate:  $0.01 \text{ V s}^{-1}$ , temperature:  $20 \pm 1 \text{ }^\circ\text{C}$ .

### 3.2. Durability investigation of Pt/C catalyst at thin-film electrode

CV technique was used to determine the Pt electrochemical active surface area (EAS) for Pt/XC-72 and Pt/BP-2000 catalysts. The typical CVs for Pt/XC-72 (Fig. 4a) and Pt/BP-2000 (Fig. 4b) catalysts were recorded before and after 1200 potential cycles. Fine structures of hydrogen adsorption/desorption peaks clearly appeared in the figure. A reduction peak centered at  $0.80 \text{ V}$  can be observed during the negative-going potential sweep. This reduction peak can be attributed to the reduction of platinum oxide. This feature curve is consistent with those of the cyclic voltammograms for Pt electrodes.

Durability investigation of the Pt/C catalyst was carried out by measuring EAS during the potential cycling test. The potential cycles were from  $0.6$  to  $1.2 \text{ V}$  at  $50 \text{ mV s}^{-1}$  in  $0.5 \text{ mol L}^{-1} \text{ H}_2\text{SO}_4$ . EAS of the catalysts could be estimated from the coulombic charge for the hydrogen adsorption and desorption ( $Q_H$ ) in the cyclic voltammograms (Fig. 4). The value of  $Q_H$  is calculated as the mean value between the amounts of charge transfer during the electro-adsorption and desorption of  $\text{H}_2$  on

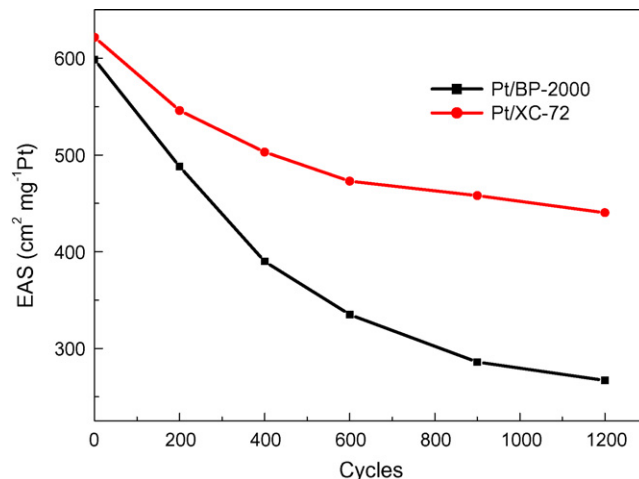


Fig. 5. Electrochemical active surface area as a function of cycle numbers of on Pt/XC-72 and Pt/BP-2000 thin-film electrodes.

Pt sites [28].

$$\text{EAS} = \frac{Q_H}{[\text{Pt}] \times 0.21} \quad (1)$$

Where  $[\text{Pt}]$  represents the platinum loading ( $\text{mg cm}^{-2}$ ) in the electrode,  $Q_H$  is the charge for hydrogen desorption ( $\text{mC cm}^{-2}$ ) and  $0.21$  represents the charge required to oxidize a monolayer of  $\text{H}_2$  on bright Pt [29].

Fig. 5 shows the EAS as a function of the cycle number obtained for different catalysts. As shown in Fig. 5, the initial EAS of Pt/XC-72 before potential cycling test is slightly higher than that of Pt/BP-2000, which is the result of the smaller Pt nanoparticle size of Pt/XC-72. Previous reports indicate that BP-2000 has large mesoporous area and dibutylphthalate (DBP) adsorption value [14], which result in high surface tension between aqueous solution and the surface of carbon particle. And the large surface tension decreases Pt dispersion uniformity. Thus, the mean Pt particle size of Pt/BP-2000 is larger than that of Pt/XC-72. In our study, the Pt particle sizes of the two catalysts were characterized by XRD, and the result will be discussed in the following. It is consistent with those of previous reports [14]. Furthermore, from the results of Fig. 5, it can be seen that the EAS of the Pt catalysts decreases with the increase of the number of cycles. After 1200 potential cycles, the EAS decreases from  $621.6$  to  $440.4 \text{ cm}^2 \text{ mg}^{-1} \text{ Pt}$  for Pt/XC-72 (by 29.2%), and from  $598.6$  to  $267 \text{ cm}^2 \text{ mg}^{-1} \text{ Pt}$  for Pt/BP2000 (by 55.4%). Thus the degradation rate of the Pt/BP-2000 catalyst is larger than that of the Pt/XC-72 catalyst.

### 3.3. ADT and physical characterization of Pt/C catalyst

To further investigate the degradation of the two catalysts, ADT was carried out at GDE by potentials cycling between  $0.6$  and  $1.2 \text{ V}$ , which caused surface oxidation/reduction cycles of Pt. We conducted the test by applying potential sweeps at the rate of  $50 \text{ mV s}^{-1}$  to the GDE in a  $0.05 \text{ mol L}^{-1} \text{ H}_2\text{SO}_4$  solution at room temperature. After 10,000 cycles, changes of the EAS in

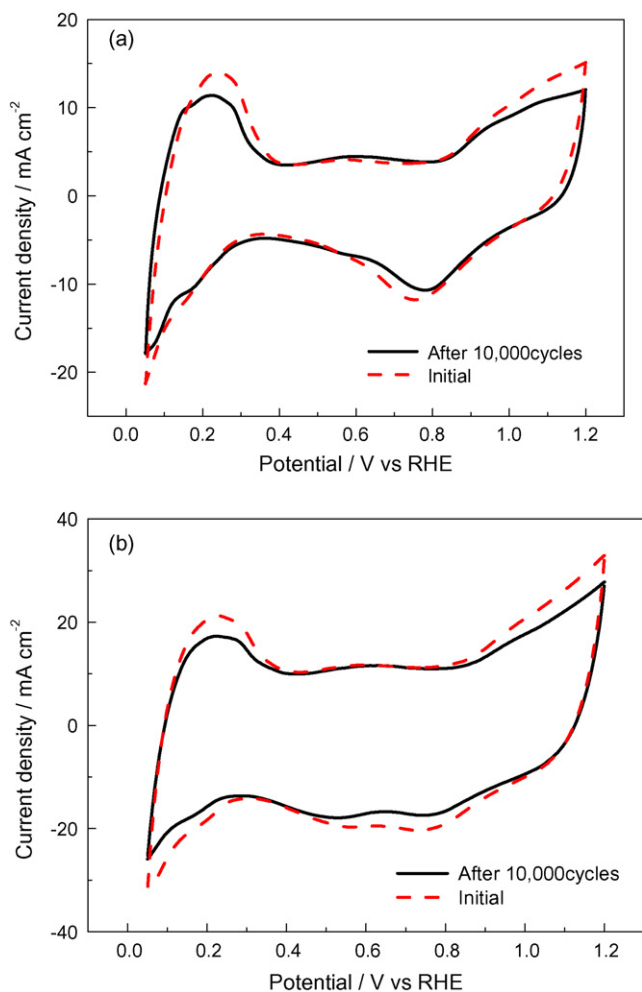


Fig. 6. Cyclic voltammograms recorded at  $0.01 \text{ V s}^{-1}$  on Pt/XC-72 (a) and Pt/BP-2000 (b) gas diffusion electrode before and after 10,000 potential cycles. The potential cycles were from 0.6 to 1.2 V in  $0.5 \text{ mol L}^{-1} \text{ H}_2\text{SO}_4$  (Ar feed), scan rate:  $0.05 \text{ V s}^{-1}$ , temperature:  $20 \pm 1 \text{ }^\circ\text{C}$ .

the catalyst and Pt oxidation states on the support surface were determined.

Fig. 6 shows CVs for the Pt/XC-72 and Pt/BP-2000 after consecutive cycling test. It can be seen that a reduction of the hydrogen adsorption and desorption in the CVs appeared on all catalysts with the potential cycling, which shows a decrease of the EAS and an increase of the Pt particle size on each catalyst. EAS of the catalyst could be estimated from the coulombic charge for the hydrogen adsorption and desorption ( $Q_H$ ) in the cyclic voltammograms as discussed above. The calculated result reveals that EAS of the Pt/XC-72 GDE (Fig. 6a) decreases from  $4383.5$  to  $3480.4 \text{ cm}^2$  (the EAS is expressed with regard to the GDE area  $2.3 \times 2.3 \text{ cm}^2$ , but not in  $\text{cm}^2 \text{ mg}^{-1} \text{ Pt}$ . The reason is that Pt amount is unknown for post-ADT sample due to the Pt dissolution or detachment) after 10,000 potential cycles test, a loss of 20.6%. In contrast, EAS of the Pt/BP-2000 GDE (Fig. 6b) decreases from  $4005.2$  to  $2363.4 \text{ cm}^2$ , a loss of 40.9%. This also confirms that Pt/XC-72 is more stable than Pt/BP-2000 in this case. The result is in agreement with that of durability investigation on thin-film electrode.

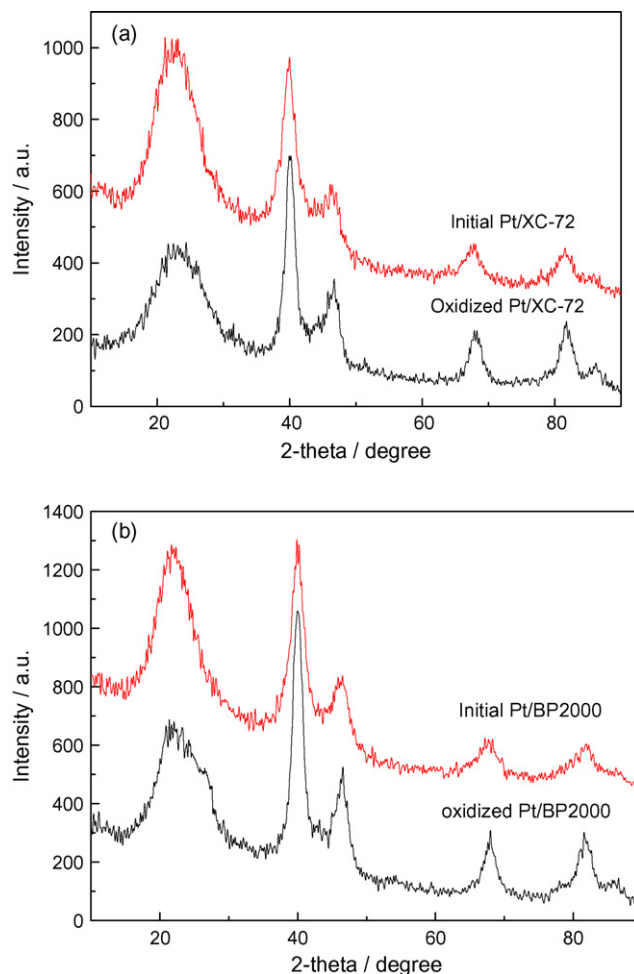


Fig. 7. XRD patterns of Pt/XC-72 (a) and Pt/BP-2000 (b) catalysts before and after 10,000 potential cycles test.

XRD patterns of the Pt/XC-72 and Pt/BP-2000 catalysts before and after 10,000 potential cycling tests were shown in Fig. 7a and b, respectively. The XRD pattern of the initial sample was taken using the received catalyst. In the case of the oxidized sample, the XRD pattern was obtained using the powders scratched from the GDE. The diffraction peak at  $2\theta$  of  $25^\circ$  shown in the catalysts is associated with the (002) plane of the hexagonal structure characteristic of carbon black. Pt nanoparticles are crystalline, as indicated by the characteristic peaks in the pattern. The diffraction peaks at  $2\theta$  of 40, 47, and 67 are associated with the Pt (111), (200), and (220) planes, respectively [30]. The mean particle sizes can be calculated according to Scherrer's formula [31]. The calculated average particle size according to the diffraction peaks of Pt(111) is 2.7, 3.7, 2.9, and 4.2 nm for original Pt/XC-72, post-ADT Pt/XC-72, original Pt/BP-2000, and post-ADT Pt/BP-2000, respectively. It can be seen that the Pt/BP-2000 catalyst presents lower sintering resistance.

The elements on the surfaces of the two catalysts were characterized by XPS. Fig. 8a–d shows Pt4f XPS spectra of Pt/XC-72 and Pt/BP-2000 catalysts before and after 10,000 potential cycling tests, respectively. The results given in percentage of total intensity were shown in Table 1. It can be seen

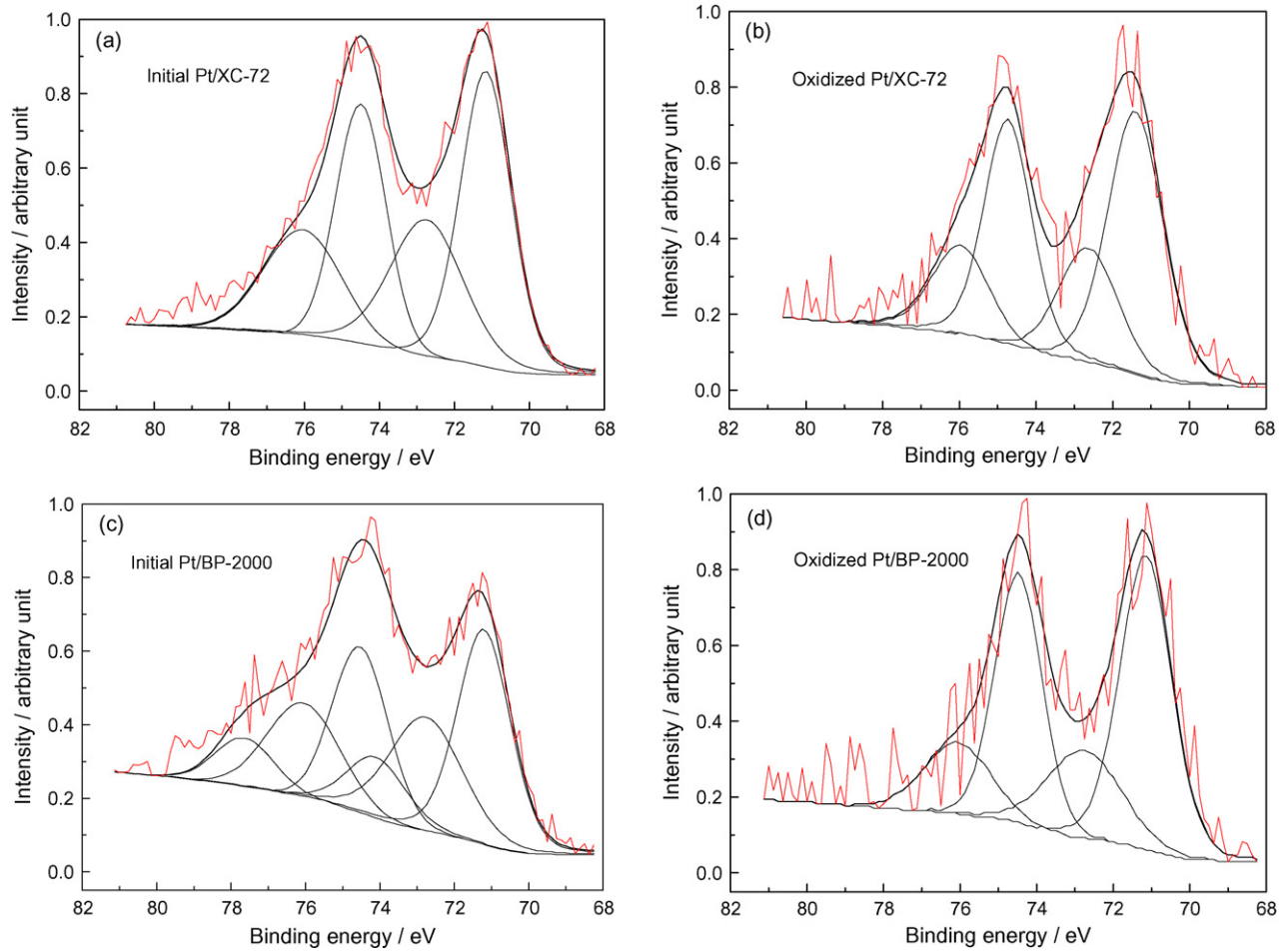


Fig. 8. Pt4f XPS spectra of initial Pt/XC-72 (a); oxidized Pt/XC-72 (b); initial Pt/BP-2000 (c); and oxidized Pt/BP-2000 (d) catalysts.

that a decrease in Pt 4f concentration appears for each catalyst after ADT. This suggests that Pt dissolved or detached from the surface of Pt/C catalyst after ADT. It can be seen that the loss of Pt amount in Pt/BP-2000 (from 2.0% to 0.5%, a decrease of 75%) is higher than that in Pt/XC-72 (from 2.4% to 0.8%, a decrease of 67%). The higher Pt amount loss results in higher EAS decrease for Pt/BP-2000 catalyst. It should be noted that the quantitative relationship between the Pt amount loss and the decrease in EAS of the catalyst is not consistent. This is because the XPS technique detects only the top 2–10 atom layer on the catalyst surface where the Pt amount loss is the highest. Thus the Pt amount loss obtained by XPS technique is larger than the EAS loss amount of the Pt/C catalyst.

It is believed that the EAS loss of Pt based catalyst is due to the following two processes: (1) Dissolution of Pt from the small particles and recrystallization into a large particle. The phenomenon is known as Ostwald ripening [32]. (2) Aggregation of adjacent small Pt nanoparticles by thermal motion in PEMFC operation process [33]. Pt dissolution and agglomeration contribute significantly to the fuel cell performance degradation. Note that the degradation of carbon support amount in the Pt/BP-2000 (from 93.1% to 69.3%) is also more severe than that of the Pt/XC-72 (from 93.4% to 76.9%). Higher carbon support corrosion occurs, higher Pt amount loss does. Thus, it can be concluded that carbon support corrosion accelerates the Pt dissolution or detachment. At the same time, the original porous

Table 1  
Results of the fits of the XPS spectra, values given in percentage of total intensity

Catalysts	Concentration (%)				Pt 4f (%)		
	Pt 4f	C 1s	O 1s	F 1s	Pt(0) species	Pt(II) species	Pt(IV) species
Initial Pt/XC-72	2.4	93.4	4.2	0	59.4	40.6	0
Oxidized Pt/XC-72	0.8	76.9	7.0	15.3	67.9	32.1	0
Initial Pt/BP-2000	2.0	93.1	4.9	0	50.0	35.6	15.4
Oxidized Pt/BP-2000	0.5	69.3	8.7	21.5	69.9	30.1	0

structure of carbon will collapse after the support corrosions, which will result in a high mass transport loss in the catalyst layer.

Fig. 8 also shows the Pt 4f XPS spectra of the two catalysts before and after ADT. It can be seen that there are different Pt states in the catalysts. The most intense doublet (71.4 and 74.7 eV) is due to metallic Pt. The second set of doublets (72.6 and 75.9 eV) could be assigned to the Pt (II) chemical state as PtO. The third doublet of Pt is the weakest in intensity, and occurred at even higher binding energies (74.3 and 77.7 eV). These are the indications that they are most likely caused by a small amount of Pt (IV) species on the surface. The XPS data of the catalysts were summarized in Table 1. During the ADT by applying potential sweeps from 0.6 to 1.2 V, oxidation–reduction cycles of Pt take place on the catalyst surface. As shown in Table 1, the amount of PtOx is reduced for each catalyst sample after ADT because the electrode potential was negatively going to 0.6 V. Note that the amount of PtOx on the surface of initial Pt/BP-2000 is higher than that of initial Pt/XC-72 catalyst, which may be the result of a higher concentration of oxygen species appeared on the surface of initial BP-2000 carbon black support, as discussed above. It is well known that the surface reaction involves the formation of PtOH and PtO derived from the oxidation of water that causes the dissolution of Pt via Pt oxidation state [7]. Thus the higher amount of PtOx on the initial Pt/BP-2000 catalyst will result in a higher Pt dissolution amount of the Pt/BP-2000 catalyst during ADT. This gives further evidence for the correlation between the stability of Pt/C catalyst and carbon support corrosion.

Carbon support with high surface area in PEMFC electrode is susceptible to corrosive conditions. If the support is oxidized to CO<sub>2</sub>/CO, Pt may be lost from the support, so the more the carbon support is oxidized, the more Pt is lost. If the support is partially oxidized to surface oxide, it may accelerate the increase of Pt particle size, because the presence of surface oxides may weaken the platinum–support interaction, leading to a lower resistance to surface migration of Pt particles [34–36]. From the above result of carbon support corrosion investigation, it can be seen that BP-2000 carbon black is easier to be oxidized under PEMFC operation process, which contribute significantly to the degradation of Pt/BP-2000 catalyst. By comparing the corrosion of the two carbon black materials with similar characteristics and structures, a good correlation was observed between carbon surface area and corrosion rate. The higher the surface area is, the more the support corrosion does. When the surface area of carbon black support increases, the microporous, mesoporous area and pore volume of the support will increase. Furthermore, more amorphous carbon with regard to plain graphite carbon may appear in the carbon material. These may be the main reasons for the low corrosion resistance of BP-2000.

#### 4. Conclusion

The durability of Pt/C catalysts with different carbon black supports (XC-72 and BP-2000) were investigated under simulated PEMFC conditions. The carbon supports were investigated by applying a fixed potential of 1.2 V. Electrochemical study and

XPS analysis indicated that BP-2000 had a lower corrosion resistance than that of XC-72. A potential cycling test from 0.6 to 1.2 V was applied to the system to investigate the disabilities of Pt/C catalysts. A higher increase of Pt particle size and a higher Pt amount loss appeared on the Pt/BP-2000 catalyst, compared with that of Pt/XC-72. Furthermore, the electrochemical measurement indicated a higher EAS degradation rate (40.9%) for Pt/BP-2000 after ADT, while it was 20.6% for Pt/XC-72 catalyst. The higher degradation rate of Pt/BP-2000 catalyst mainly resulted from the lower corrosion resistance of BP-2000.

#### Acknowledgement

This work was supported financially by Natural Science Foundation of China (No. 20476020 and 20606007).

#### References

- [1] X. Cheng, L. Chen, C. Peng, Z. Chen, Y. Zhang, Q. Fan, *J. Electrochem. Soc.* 151 (2004) 48.
- [2] S.D. Knights, K.M. Colbow, J. St-Pierre, D.P. Wilkinson, *J. Power Sources* 127 (2004) 127.
- [3] D.A. Stevens, M.T. Hicks, G.M. Haugen, J.R. Dahn, *J. Electrochem. Soc.* 152 (2005) 2309.
- [4] M.S. Wilson, F.H. Garzon, K.E. Sickafus, S. Gottesfeld, *J. Electrochem. Soc.* 140 (1993) 2872.
- [5] E. Antolini, *J. Mater. Sci.* 38 (2003) 2995.
- [6] L.M. Roen, C.H. Paik, T.D. Jarvi, *Electrochem. Solid-State Lett.* 7 (2004) 19.
- [7] J. Zhang, K. Sasaki, E. Sutter, R.R. Adzic, *Science* 315 (2007) 220.
- [8] H.R. Colon-Mercado, B.N. Popov, *J. Power Sources* 155 (2006) 253.
- [9] X.P. Wang, R. Kumar, D.J. Myers, *Electrochem. Solid-State Lett.* 9 (2006) 225.
- [10] R.M. Darling, J.P. Meyers, *J. Electrochem. Soc.* 126 (2003) 1523.
- [11] Y.Y. Shao, G.P. Yin, J. Zhang, Y.Z. Gao, *Electrochim. Acta* 51 (2006) 5853.
- [12] Y.Y. Shao, G.P. Yin, Y.Z. Gao, P.F. Shi, *J. Electrochem. Soc.* 153 (2006) 1093.
- [13] X. Wang, W.Z. Li, Z.W. Chen, M. Waje, Y.S. Yan, *J. Power Sources* 158 (2006) 154.
- [14] G.X. Wang, Q. Sun, Z.H. Zhou, J.G. Liu, Q. Wang, S. Wang, J.S. Guo, S.H. Yang, Q. Xin, B.L. Yi, *Electrochem. Solid-State Lett.* 8 (2005) 12.
- [15] P. Yu, M. Pemberton, P. Plasse, *J. Power Sources* 144 (2005) 11.
- [16] M.F. Mathias, R. Makharia, H.A. Gasteiger, J.J. Conley, T.J. Fuller, C.J. Gittleman, S.S. Kocha, D.P. Miller, C.K. Mittelsteadt, T. Xie, S.G. Yan, P.T. Yu, *Interface* 14 (2005) 24.
- [17] R. Makharia, S. Kocha, P. Yu, M.A. Sweikart, W. Gu, F. Wagner, H.A. Gasteiger, *ECS Trans.* 1 (2006) 3.
- [18] R.L. Borup, J.R. Davey, F.H. Garzon, D.L. Wood, M.A. Inbody, *J. Power Sources* 163 (2006) 76.
- [19] Z.B. Wang, G.P. Yin, P.F. Shi, Y.C. Sun, *Electrochem. Solid-State Lett.* 9 (2006) 13.
- [20] J.H. Tian, F.B. Wang, Z.Q. Shan, R.J. Wang, J.Y. Zhang, *J. Appl. Electrochem.* 34 (2004) 461–467.
- [21] T.J. Schmidt, H.A. Gasteiger, G.D. Stab, P.M. Urban, D.M. Kolb, R.J. Behm, *J. Electrochem. Soc.* 145 (1998) 2354.
- [22] H.R. Colon-Mercado, H. Kim, B.N. Popov, *Electrochem. Commun.* 6 (2004) 795.
- [23] K.H. Kangasniemi, D.A. Condit, T.D. Jarvi, *J. Electrochem. Soc.* 151 (2004) E125.
- [24] J.S. Ye, X. Liu, H.F. Cui, W.D. Zhang, F.S. Sheu, T.M. Lim, *Electrochem. Commun.* 7 (2005) 249.
- [25] J.H. Chen, W.Z. Li, D.Z. Wang, S.X. Yang, J.G. Wen, Z.F. Ren, *Carbon* 40 (2002) 1193.

- [26] J.L. Figueiredo, M.F.R. Pereira, M.M.A. Freitas, J.J.M. Orfao, *Carbon* 37 (1999) 1379.
- [27] T.C. Kuo, R.L. McCreery, *Anal. Chem.* 71 (1999) 1553.
- [28] A. Pozio, M.D. Francesco, A. Cemmi, F. Cardellini, L. Giorgi, *J. Power Sources* 105 (2002) 13.
- [29] F. Maillard, M. Martin, F. Gloaguen, J.M. Leger, *Electrochim. Acta* 47 (2002) 3431.
- [30] M. Carmo, V.A. Paganin, J.M. Rosolen, E.R. Gonzalez, *J. Power Sources* 142 (2005) 169.
- [31] V. Radmilovic, H.A. Gasteiger, P.N. Ross, *J. Catal.* 154 (1995) 98.
- [32] M. Watanabe, K. Tsurumi, T. Mizukami, T. Nakamura, P. Stonehart, *J. Electrochem. Soc.* 141 (1994) 2659.
- [33] M. Uchida, Y. Aoyama, M. Tanabe, N. Yanagihara, N. Eda, A. Ohta, *J. Electrochem. Soc.* 142 (1995) 2572.
- [34] F. Coloma, A. Sepulvedaescribano, J.L.G. Fierro, F. Rodriguez-Reinoso, *Langmuir* 10 (1994) 750.
- [35] M. Kang, Y.S. Bae, C.H. Lee, *Carbon* 43 (2005) 1512.
- [36] A. Guerrero-Ruiz, P. Badenes, I. Rodriguez-Ramos, *Appl. Catal. A* 173 (1998) 313.